A Theoretical and Experimental Analysis of Variances in Weld Bead Morphologies

M. Marya and S.K. Marya

(Submitted 20 August 1997; in revised form 25 February 1998)

Predictable and reproducible weld bead morphologies and dimensions are a major concern in welding. In bead-on-plate welding, the heat flow is controlled by the heat source parameters (power, speed, and radius) and the physical properties and dimensions of the workpiece, especially its thickness. Complex models that account for weld pool circulation have been developed to quantify welds. However, to some extent, fluctuations in weld dimensions can be explained with conduction models of moving Gaussian heat sources. In early investigations with point and line heat sources, relationships between process parameters and plate thickness were derived to differentiate between two- and three-dimensional heat flow. To date, the heat source radius (*R*) has not been taken into account. The dimensionless ratio (*D) of the plate thickness (*D*) to the heat source radius (*R*) is actually a variable to consider. With the introduction of additional dimensionless parameters (*)—speed (*v**), power (*q**)—relationships among governing variables, heat flow dimension, and weld bead dimensional fluctuations can be derived. Weld bead fluctuations are found to depend on dimensionless variables (*v**, *q**, *D**) and occur when the heat flow dimension is intermediate between two- and three- dimensional. Occasionally, experimental data exhibit trends that differ from predictions. This article presents a dimensionless version of a heat flow model and discusses the discrepancies between experimental and theoretical results.**

Keywords GTA welding, modeling, 2D/3D heat flow, weld pool dynamics

1. Introduction

The shape and dimensions of weld beads are governed by complex convective flows (Ref 1, 2) of the molten metal, heat conduction within the base material, and, to a lesser extent, within the weld pool. Despite huge advances in computational techniques, the simulation of fusion welding processes remains quite imprecise for several reasons. For instance, convection is mainly controlled by surface tension gradients within the weld pool promoted by compositional and temperature gradients. In welding conditions, surface tension values are poorly known because any variation of weld pool composition, even insignificant, may change entirely the magnitude and sign of the surface tension gradient (Ref 3-7). Without accurate data on the weld pool chemistry, even an extremely sophisticated model would be unable to produce accurate predictions. However, a number of weld bead characteristics can be identified and quantified with relatively simple analysis. For example, explanations on weld shape and size fluctuations can be provided with analytical models based only on heat conduction.

From a practical standpoint, a weld bead with dimensional variations is unacceptable because it leads to nonuniform mechanical properties along the weld joint. To maintain a uniform joint, weld bead dimensions such as penetration depth, front bead width, and back bead width (for complete joint penetration) must be held constant. Such constancy is sometimes hard to achieve, especially near complete joint penetration where significant shape and dimensional variations are commonly observed. Variations in the net heat input to the workpiece must be at the origin of these unexpected changes. Weld bead instability has also been reported in the welding of plates of variable thickness (Ref 8) where relatively unanticipated penetration depths have been obtained. The backside of the plate clearly plays a

M. Marya, formerly with ECN, now with Colorado School of Mines, Center for Welding, Joining and Coatings Research, Golden, Colorado, USA; and **S.K. Marya,** Laboratoire Mécanique et Matériaux, Ecole Centrale de Nantes (ECN), Nantes, France.

Nomenclature

T	Temperature, °C
T_0	Initial temperature, °C
T_m	Melting temperature, °C
q	Heat source/welding power, W
v	Welding speed, m/s
η	Heat source efficiency
n	Operating parameter (three-dimensional heat flow)
τ	Relative plate thickness, m^{-1}
a	Thermal diffusivity, m^2/s^{-1}
λ	Thermal conductivity, $J/m^{-1}/s^{-1}/°C^{-1}$
ρC_p	Specific heat, $J/m^{-3}/°C^{-1}$
σ	Heat source distribution parameter
R	Heat source radius, m
t	Time, s
x, y, z	Cartesian coordinates, m
D	Plate thickness, m
W_f	Front weld/bead width, m
W_b	Back weld/bead width, m
Z_m	Weld penetration, m
*	Refers to dimensionless parameters

primary role when approaching melting. It acts as a heat or thermal barrier whose effect is to reorient the incoming heat flow back to the weld pool. Its effect is progressive and becomes significant only when a certain threshold of process parameters, determined later, is reached. Once attained, abrupt changes in weld bead penetration and width are likely to occur. In this article, interactions among processing variables (heat source power, speed, and size), material thermal properties (thermal conductivity, thermal diffusivity, and melting temperature), and plate thickness are studied to identify conditions where heat flow fluctuations are particularly critical. Data from the gas tungsten arc welding (GTAW) of two very low thermal conductors—Inconel 625 and Ti-6Al-4V—are also provided for comparisons with the theoretical predictions of weld bead dimensions.

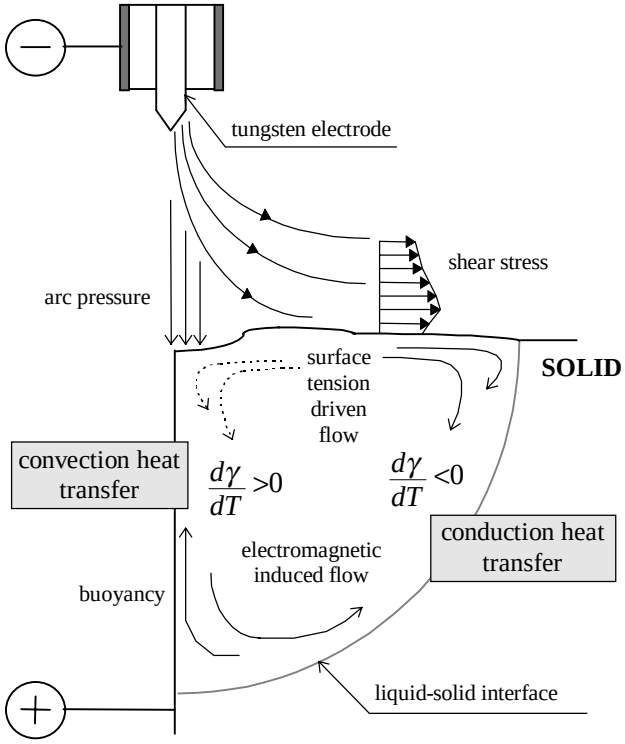

Fig. 1 Review of the major forces controlling the heat transfer and the weld bead morphology in gas tungsten arc

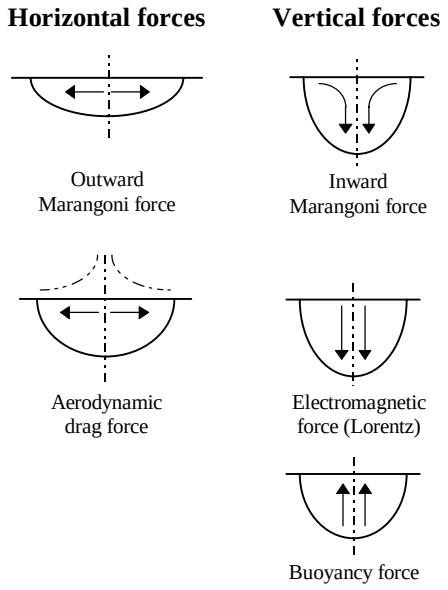

Fig. 2 Various driving forces involved in arc welding and their individual effect on the weld pool dynamics. Source: Ref 4, 11

The above discussion suggests that weld bead fluctuations, which result from heat flow changes, originate from three distinct causes: 1) variations in heat source intensity, possibly resulting from unexpected alterations in arc length or heat input; 2) geometrical changes that promote uneven edge or thickness and perturb the quasi-steady state heat flow; or 3) the presence of minor elements in the weld pool. In this article, the first two causes are explained with a conduction model of a moving Gaussian heat source. In contrast, the third cause is mainly clarified on the basis of differences observed between experimental and calculated trends. As a general rule, experimental trends that deviate from predictions of heat conduction models can be attributed to increasingly strong weld pool convection, as discussed in the following sections.

2. Modeling

Weld bead shape and dimensions are governed by a set of equations of conservation whose complexity increases with the number of physical features that models attempt to capture (Ref 9). Nevertheless, the primary aspects of heat flow are frequently well reproduced with heat conduction models. The importance of convection, that is, heat transport by mass motion, relative to heat conduction, can be estimated from the Peclet number (Pe), which is defined by the relation: $Pe = (vL\rho C_p)/\lambda$ where L is a characteristic length (generally taken as half the surface weld width), ρ is the molten metal density, C_p is the molten metal specific heat, λ is the molten metal thermal conductivity, and v is the molten metal velocity (usually considered at the pool surface). It is accepted that the heat flow is essentially controlled by convection when the Peclet number exceeds 10 (Ref 10).

Bless (Ref 10) analyzed the problem of convection for simple weld pool shapes and derived the following equation for predicting the fluid-flow velocity: $v = F/G\mu$ where F is the driving force, G is a factor (dependent upon the geometry of the pool and usually very close to 20), and μ is the fluid viscosity. As shown in Fig. 1 and 2, the forces that drive the motion of molten metal in the weld pool in arc welding are: the buoyancy force (density difference in the liquid metal), the Lorentz electromagnetic force (dominant at elevated currents), the aerodynamic drag force (shear stress), the arc pressure, and the surface tension or Marangoni force (flow driven by surface tension). On the basis of weldability studies in stainless steels, Heiple and Roper (Ref 12) proposed that the surface tension gradient is usually the dominant driving force. Experimental confirmation of the validity of the surface tension driven flow model comes from Mills et al. (Ref 13), who measured surface tension values as a function of temperature for stainless steels exhibiting both good and poor weld penetrations. With only the surface-tension-driven flow in view, the previous veloc-

ity-force equation can be rewritten as: $v = (-d\gamma/dT)(T_{max} - T_{min})/G\mu$. A positive value of velocity indicates that the molten metal is flowing outward, that is, from the pool center toward the edge. A Marangoni flow that occurs in the direction of the heat extraction, that is, down the temperature gradient, characterizes materials with negative coefficients of surface tension ($d\gamma/dT$). Actually, most alloys exhibit negative $d\gamma/dT$ (the surface tension decreases with increasing temperature). However, in the presence of relatively small amounts of surface active elements (for iron, the elements are: oxygen, sulfur, phosphorus, or selenium), $d\gamma/dT$ can become positive within a limited temperature range. The resulting Marangoni flow is directed inward and downward, promoting high weld aspect ratios (Z_m/W_f, where Z_m is weld penetration and W_f is front weld width).

In general, heat flow in a weld pool is dominated by convection (Ref 1, 2). Nevertheless, under special circumstances, as in the presence of lower temperature gradients (as a result of heat input changes) and additional contributions from surface active elements, the overall force balance within the weld pool can be deeply reduced, thus decreasing the fluid velocity, the Peclet number, and the relative importance of convection with respect to conduction. As conduction becomes more dominant, conduction models naturally gain validity. However, in many practical cases where the heat flow is convective within the weld pool, welds exhibit circular or elliptical shapes in cross section. The thermal fields calculated from heat conduction and produced by moving point, line, cylindrical, or Gaussian heat sources, are made of isotherms of elliptical form. Therefore, they are totally capable of reproducing weld bead shapes, even though the fundamental mechanism describing the heat transfer is different. For a few cases, point heat source or line heat source solutions, commonly designated as Rosenthal equations (Ref 14), can predict reasonably well weld bead dimensions. In many situations, a Gaussian or a combination of heat sources is however more appropriate (Ref 15, 16). Elmer et al. (Ref 17) have found that the applicability of these models is dependent upon the source intensity, or energy density. In general, the point heat source is more suitable for low-intensity welding where weld beads approximate semicircles ($Z_m/W_f \approx 1/2$). On the contrary, the line heat source would be preferred with high-intensity processes where weld bead aspect ratios are large. Due to its adjustable heat flux distribution, the Gaussian source is more versatile and can cover a larger range of intensities. In the model proposed by Eager and Tsai (Ref 15), which is adopted in this study, the Gaussian source illustrated in Fig. 3 must be calibrated with parameters that take into account its efficiency (η) and its heat distribution (R). As in some early models, their solution is also established for constant physical properties and adiabatic surfaces. Once rearranged to incorporate the plate thickness using a method of images, it can be presented as follows:

$$T(x,y,z,t) = T_0 + \sum_{k=-\infty}^{+\infty} \frac{q(x,y)}{\pi \cdot \rho C_p} \times \int_{t_{i'}}^{t} \frac{[\pi \cdot a \cdot (t-t')]^{-1/2}}{4 \cdot a \cdot (t-t') + R^2} \cdot \exp\left[-\frac{(x+v\cdot t)^2 + (y)^2}{4 \cdot a \cdot (t-t') + R^2} - \frac{(z+2\cdot k\cdot D)^2}{4 \cdot a \cdot (t-t')}\right] \cdot dt' \quad \text{(Eq 1)}$$

where

$$q(x,y) = \frac{\eta \cdot q}{\pi \cdot R^2} \exp\left(-\frac{x^2+y^2}{R^2}\right) \quad \text{(Eq 2)}$$

In agreement with the dimensionless approach proposed by Christensen (Ref 18) to treat the Rosenthal equations, Eager and Tsai (Ref 15) normalized their solution to include the operating parameter (n), defined as: $n = (qv)/[4\pi a^2 \rho C_p (T_m - T_0)]$ for a three-dimensional heat flow. However, the operating parameter contradicts common sense as it depends on the product of two variables, welding power and welding speeds, which produce opposite effects. In this study, welding power and welding speed have been uncoupled to avoid any ambiguities. From dimensionless works of Kou (Ref 19), and later Shercliff and Ashby (Ref 20) and Marya (Ref 21), different dimensionless parameters are suggested:

Dimensionless temperature:

$$T^* = \frac{T - T_0}{T_m - T_0} \quad \text{(Eq 3)}$$

Dimensionless time:

$$t^* = \frac{t}{t_0} \text{ with } t_0 = \frac{R^2}{4 \cdot a} \quad \text{(Eq 4)}$$

Dimensionless speed:

$$v^* = v \cdot \frac{R}{a} \quad \text{(Eq 5)}$$

Dimensionless power:

$$q^* = \frac{q}{R \cdot \lambda \cdot (T_m - T_0)} \quad \text{(Eq 6)}$$

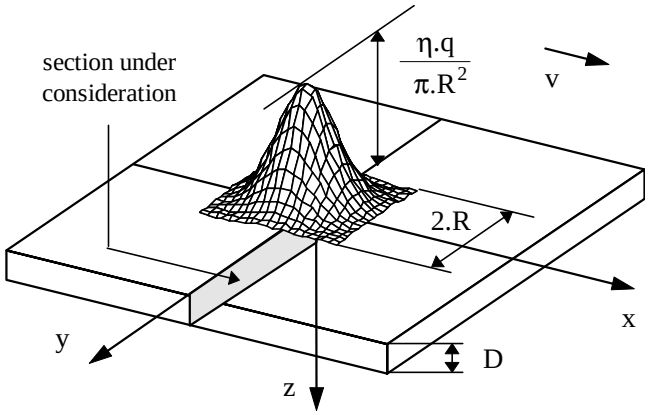

Fig. 3 Coordinate system and heat source description as used for the heat flow analysis

Dimensionless coordinates:

$$(x^*,y^*) = \left(\frac{x}{R}, \frac{y}{R}\right) \quad \text{(Eq 7)}$$

Dimensionless plate thickness:

$$D^* = \frac{D}{R} \quad \text{(Eq 8)}$$

Substituting the dimensionless parameters described in Eq 3 to 8 in Eq 1, the following dimensionless solution for calculating the temperature field due to a moving Gaussian heat source in a plate of thickness (D) is eventually derived:

$$T(x^*,y^*,z^*,t^*)^* = \sum_{k=-\infty}^{+\infty} \frac{q^*}{2 \cdot \pi \cdot \sqrt{\pi}} \times \int_{t_i^*}^{t^*} \frac{1}{[(t^* - t'^*) + 1]) \cdot \sqrt{t^*}} \cdot \exp$$

$$[-\frac{(x^* + v^* \cdot t'^*/4)^2 + (y^*)^2}{(t^* - t'^*) + 1} - \frac{(z^* + 2 \cdot k \cdot D^*)^2}{(t^* - t'^*)}] \cdot dt'^* \quad \text{(Eq 9)}$$

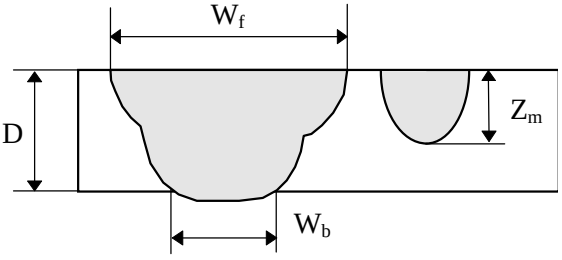

Fig. 4 Characteristic dimensions of weld beads (cross-section representation)

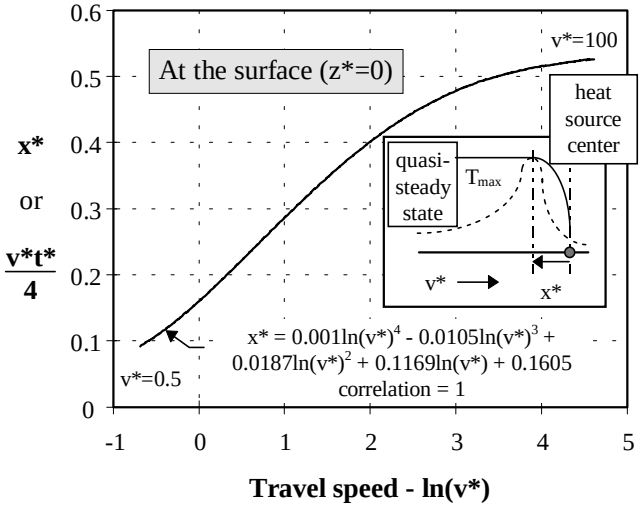

Fig. 5 Influence of the welding speed (v^*) on the distance (x^*) at which the surface temperature (T^*) reaches its maximum value

3. Analysis

The elimination of the time variable from the heat flow solutions allows finding, in quasi-steady state ($t^* \rightarrow \infty$), helpful relations between the dimensionless processing parameters (q^*,v^*) and their effects (Z_m^*,W_f^*,W_b^*) where Z_m, W_f, and W_b refer to weld bead dimensions, as illustrated in Fig. 4. These characteristics, Z_m^*, W_f^*, and W_b^*, are iteratively calculated, and their final values are given when their associated peak temperatures (T^*) equal one. This peak temperature is reached at a precise time (t^*) during which the heat source had moved away from its initial location ($x^* = 0$, $t^* = 0$) by a distance (x^*). Evidently, dimensionless time and distance can be related by the relation $v^* = 4x^*/t^*$ that can be deduced from Eq 4 and 5. To minimize the computation time, that is, practically the number of iterations, it is important to estimate t^* or x^*. For this purpose, the very general calculation of peak temperature at the frontside centerline ($y^* = 0$, $z^* = 0$) of a semi-infinite plate has been useful. In this particular case, the distance from the heat source center at which the peak temperature is reached is given in Fig. 5.

As shown in Fig. 5 with a three-dimensional heat flow, ($D \rightarrow \infty$) the quasi-steady state that can be characterized by an unchanging peak temperature along the centerline ($y^* = 0$, $z^* = 0$), is reached after greater distances when the welding speed (v^*) increases. As long as this stationary regime is not attained, weld bead dimensions are subject to variations. The plate thickness obviously has an important role to play on the magnitude of the transient regime that precedes the quasi-steady state. For instance, in the welding of a plate of variable thickness, the quasi-steady-state heat flow would be difficult to achieve because the heat extraction efficiency always keeps changing. In general, the plate thickness has a significant effect whenever the heat propagation within the thickness is rapid compared to the "heat source kinetics." In other words, at low welding speeds, the backside is very likely to affect the frontside that remains unable to evacuate fast enough the incoming heat. Because thermal diffusion is time dependent, high welding speeds lower the

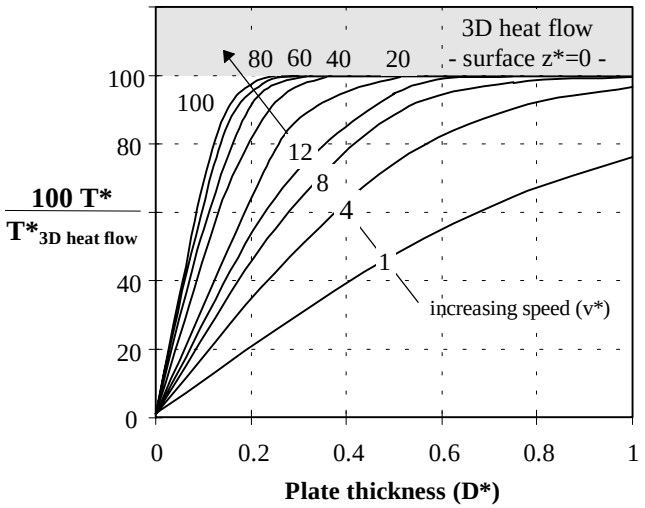

Fig. 6 Influence of the plate thickness (D^*) on the surface temperature for various speeds (v^*)

backside influence on the frontside temperature, as shown in Fig. 6, where steady-state frontside temperatures for various values of plate thickness and speeds are compared to temperatures obtained with a three-dimensional heat flow. As the welding speed is enhanced, the three-dimensional heat flow condition is promoted. As a consequence of these various points, high welding speeds allow the quasi-steady state to be reached after longer welding distances, but also with thinner plates, as illustrated in Fig. 5 and 6.

For a three-dimensional heat flow, that is, for welds of shallow penetration as compared to the plate thickness, a minor variation of welding speed or welding power would not have any appreciable effects. Nevertheless, in the vicinity of complete penetration ($Z_m \rightarrow D$) where the heat extraction efficiency significantly changes (from heat conduction to convection and radiation into the surroundings), the weld bead dimensions (Z_m, W_f, W_b) are more specially altered by small fluctuations in the welding parameters. In circumstances where the plate is not thick enough to act like a semi-infinite body, the weld bead sensitivity to heat flow is said to be high.

As illustrated in Fig. 7 and 8 for a constant plate thickness ($D^* = 1$), weld bead sensitivity depends on welding power (q^*) and welding speed (v^*). Because a precise definition of weld bead sensitivity does not exist, it can be interpreted and quantified by various variable combinations. The slopes of the curves presented in Fig. 7 and 8, either $dZ_m/dq^*|_{v^* = \text{const}}$ or $dZ_m/dv^*|_{q^* = \text{const}}$, are probably appropriate criteria to estimate weld bead sensitivity. At low speeds (v^*), a negligible variation of welding power (q^*), resulting from minor changes of current, voltage, or arc length, may have a considerable effect as dZ_m/dq^* remains invariably large at all depths (Z_m^*). In contrast, at high speeds (v^*), dZ_m/dq^* acquires a greater tendency to vary and increases significantly near complete penetration. In this case, the weld bead sensitivity gains importance only for relatively deep weld penetrations (Z_m^*). Likewise, and in particular for high welding powers, a minimal change of welding speed may be sufficient to noticeably modify the weld penetration as shown in Fig. 8. The minimization of process parameter fluctuations, especially when weld bead sensitivities are significant, is therefore preferable. A judicious combination of parameters (q^*, v^*, D^*) must be found to decide whether or not weld bead sensitivity is consequential.

An interesting and important feature that point heat source and line heat source solutions share in common is the unique dependence upon heat input, represented by the ratio q/v, which has dimensions of energy per unit length (J/m). These solutions suggest that the temperature increases linearly with q/v. Nevertheless, in the presence of high weld bead sensitivities, this linearity is no longer conserved, and therefore q/v should not be employed anymore. Analogously, the same discussion can be carried out for q^*, v^*, and their ratio q^*/v^*. As welding speed (v or v^*) and welding power (q or q^*) increase, the weld bead sensitivity is greatly reduced as demonstrated earlier, and q/v or its dimensionless homonym may then regain significance. In this study, further modifications are made to deal with the relative plate thickness (τ), a combination of parameters first introduced by Jhaveri et al. (Ref 22, 23).

$$\tau^* = \sqrt{\frac{v^*}{q^*}} \text{ or } \tau = R\sqrt{\frac{v\rho C_p(T_m - T_0)}{q}} \qquad \text{(Eq 10)}$$

Eq 1 and 9 do not directly indicate that q/v, and therefore τ, or their dimensionless form, are pertinent groups of variables. However, Fig. 9, which was derived from the same data as in Fig. 8, shows for any given τ^* (or q^*/v^*) that penetration depths tend toward finite identical values as welding speed increase. This suggests that the ratio (q/v) is a parameter that can be considered whenever the backside influence is negligible, that is, basically when the heat flow is three-dimensional. Figure 9 further demonstrates that the finite thickness influence is appreciable when τ^* has a value below 0.57 (for $D^* = 1$). This behavior is particularly discernible for relatively high values of q^* and v^*. According to the previous discussion, these sudden

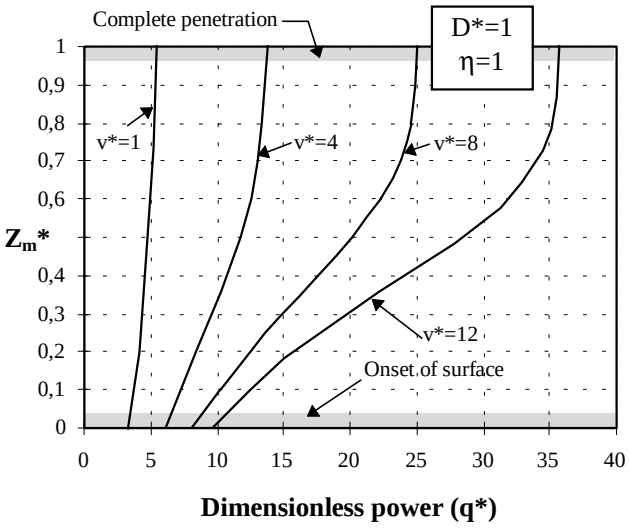

Fig. 7 Weld penetration (Z_m*) as a function of welding power (q^*) for various welding speeds (v^*)

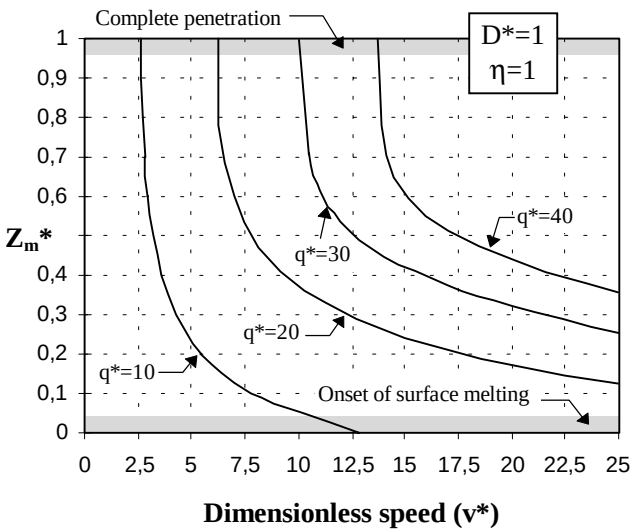

Fig. 8 Weld penetration (Z_m*) as a function of welding speed (v^*) for various welding powers (q^*)

changes of weld penetration can be clearly related to the transition between two- and three-dimensional heat flow. Jhaveri et al. (Ref 21) demonstrated using point and line heat sources that the heat flow can be treated as two-dimensional when τ is below 0.6 and three-dimensional when its value exceeds 0.9. Between these two particular values, heat flow is neither three-dimensional nor two-dimensional, but intermediate to the two regimes. As a consequence, the weld penetration sensitivity appears considerably enhanced during the transition from three-dimensional to two-dimensional heat flow.

Up to this point, focus has been on developments that deal with weld depth variations near complete joint penetration. In a like manner, the back weld width undergoes steep changes when the heat flow falls in the transition regime. The heat flow can only be considered fully two-dimensional for widths when the weld bead shape approximates a rectangular profile, that is, when W_b^* tends to equal W_t^*.

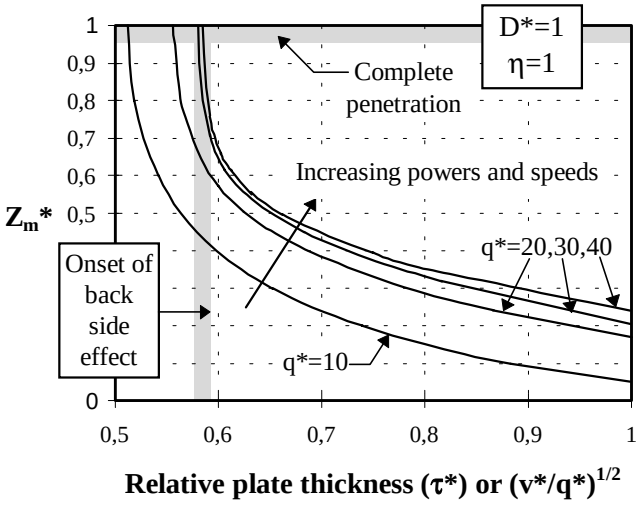

Fig. 9 Penetration (Z_m*) as a function of the relative plate thickness (τ*) or $(v^*/q^*)^{1/2}$

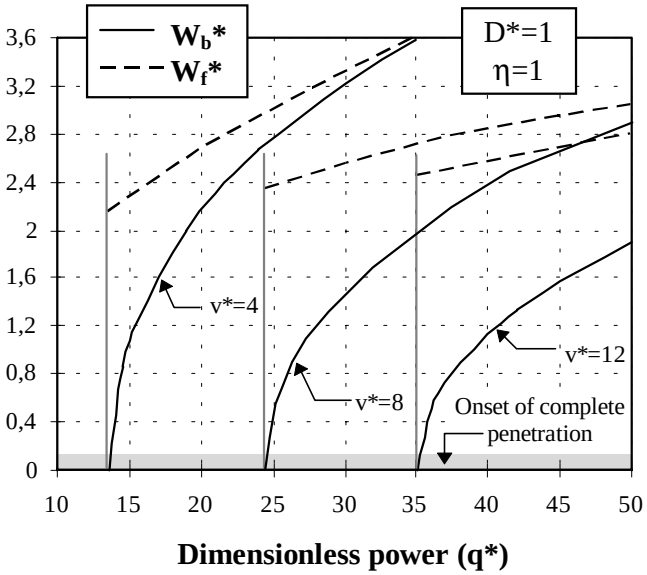

Fig. 10 Influence of (q^*) and (v^*) on the weld bead widths (W_f^* and W_b^*, melt through joints)

As illustrated in Fig. 10, the back weld width increases tremendously in the early stages of back surface melting. On the other hand, the front weld width continues to increase at a rate approximately constant; that is, $dW_f/dq*|_{v^* = \text{const}}$ is almost invariable. As in the previous analysis on penetration variations, the back weld width is more likely to fluctuate at moderate speeds, because $dW_b/dq*|_{q^* = \text{const}}$ is slightly larger.

Critical weld bead sensitivities can be estimated with weld penetrations (Z_m^*) that closely approach the plate thickness (D^*), or with back weld widths (W_b^*) that near zero, that is, with any criteria that quantifies the onset of back surface melting. Therefore, the thickness effect on the weld bead sensitivity can be investigated by calculating combinations of q^* and v^* required to trigger back surface melting. In Fig. 11, critical values of relative plate thickness are plotted as a function of the normalized plate thickness (D^*). To capture these features into an analytical form, the data from the model have been approximated by relationships determined using a least square root analysis. The computation of these data for different values of plate thickness has yielded Eq 10 and 11, which show a dependence between relative plate thickness (process parameters dependent) and various geometrical characteristics (plate thickness and heat source radius). To prevent high weld bead sensitivities, that is, a variable heat flow, values of 0.57 given by Eq 11, or of τD_{critic} provided by Eq 12 must be avoided. As expressed in Eq 12 and Fig. 12, critical weld bead sensitivities (τD_{critic}) converge to a maximum value, which indicates that the heat source size no longer has effect. In circumstances where the heat source is small as compared to the plate thickness, its size can be neglected, and the source can then be regarded as a point. This particular value where the heat source radius loses its significance belongs to the range 0.6 to 0.9 that was found to define the transition regime and is therefore in agreement with Jhaveri's analysis (Ref 22, 23).

$$\tau^* - 0.13[\ln(D^*)]^2 + 0.44[\ln(D^*)] \neq 0.57 \qquad \text{(Eq 11)}$$

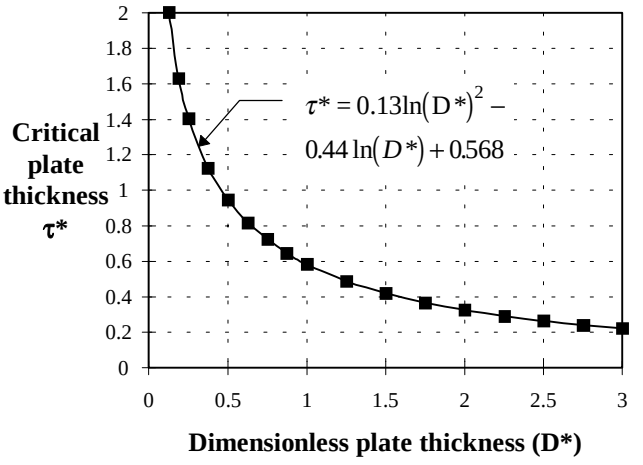

Fig. 11 Relation between relative plate thickness (τ*) and actual plate thickness (D^*) at maximum weld bead sensitivity (critical τ*)

$$(\tau D)_{critic} = 0.71 - \frac{0.12}{(D/R)} + \frac{0.12}{(D/R)} \exp\left(-5.3\,\frac{D}{R}\right) \qquad \text{(Eq 12)}$$

In the previous developments, weld bead sensitivity was described in terms of $dZ_m/dq^*|_{v^*=\text{const}}$ or $dZ_m/dv^*|_{q^*=\text{const}}$. Afterward, it was characterized by coupling welding speed (v^*) and welding power (q^*) in a parameter that has been designated as relative plate thickness (τ or τ^*). In the upcoming analysis, the process parameter is not even mentioned because focus is placed on the variation of one dimension relative to another. The ratio dW_f/dZ_m is now examined. In the case of pure heat conduction, depth (Z_m) and width (W_f) vary typically as in Fig. 13. In the presence of convection, the W_f versus Z_m curve profile can be considerably different, as discussed in the next section. At the very beginning, when both Z_m and W_f are near zero, the width increases significantly; thus dW_f/dZ_m is relatively large. The heat flow is then entirely three-dimensional and also greatly different from the circular weld shape given by the point heat source solution. As complete penetration is approached, the penetration depth of the weld increases faster than its width, which means that dW_f/dZ_m tends toward zero. These various observations have been summarized in Table 1 and illustrated in Fig. 13.

4. Experimental Developments

The weld bead sensitivity increases tremendously near the onset of back surface melting as the heat extraction mode, which is strongly controlled by the plate thickness, changes from three- to two-dimensional. When comparing several materials, much greater dependence on geometry, and in particular thickness, is expected in materials with low thermal diffusivity because of their poor ability to cool rapidly. To accentuate this behavior, engineering materials with very low thermal diffusivity such as titanium alloys (Ti-6Al-4V; $a \approx 9 \times 10^{-6}$ m^2/s) or nickel-base superalloys (Inconel 625; $a \approx 4.7 \times 10^{-6}$ m^2/s) have been selected. Their weld bead sensitivities are studied here in various ways.

Table 1 Dimensional changes in weld beads as a function of heat flow

Zone	Heat flow(a)	τD	dW_f/dZ_m
1	3D	$<<\tau D_{critic}$	High
2	3D → 2D (depth)	$<\tau D_{critic}$	Toward zero
3	3D → 2D (width)	$>\tau D_{critic}$	Zero to indefinite

τD_{critic} is given by Eq 11. (a) 3D, three-dimensional; 2D, two-dimensional

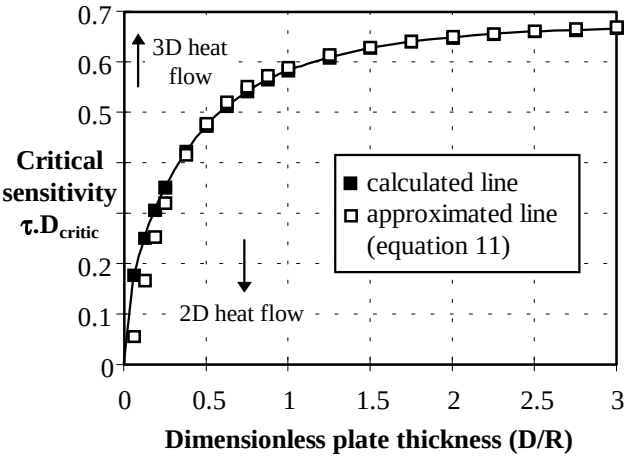

Fig. 12 Determination of weld bead sensitivities ($\tau^* D^*$ or τD) for various plate thicknesses (D^* or D/R)

Figure 14 is a dimensionless representation of some of the results as suggested by the Rosenthal equation (3D-heat flow). Weld penetration values are plotted as a function of the operating parameter(n). From the comparison of experimental data with the calculated curve (dash line), the thickness influence can clearly be detected at the lowest *n*-values. As *n* increases in response to higher welding speeds (current and voltage are held constant), the heat flow becomes three-dimensional and the experimental data fit the predictions rather well. On the contrary, as the welding speed is reduced (*n* decreases), the weld penetration becomes deeper and the theoretical curve fails to fit the experimental data. The heat flow is no longer three-dimensional, but progressively becomes two-dimensional.

Although this first analysis does not take into consideration effects of thickness and heat source size on heat flow changes, it demonstrates in a totally different way that the heat flow mechanism changes as complete penetration is approached. When looking at Fig. 9 derived from the theoretical model, the resemblance with Fig. 15 is apparent, and the weld penetration sensitivity when approaching the backside has now been experimentally established.

As expected, Inconel 625, which possesses a thermal diffusivity about half that of Ti-6Al-4V, seems to exhibit a greater weld penetration sensitivity. Figure 15 and 16 show indeed that the transition between penetration values obtained at

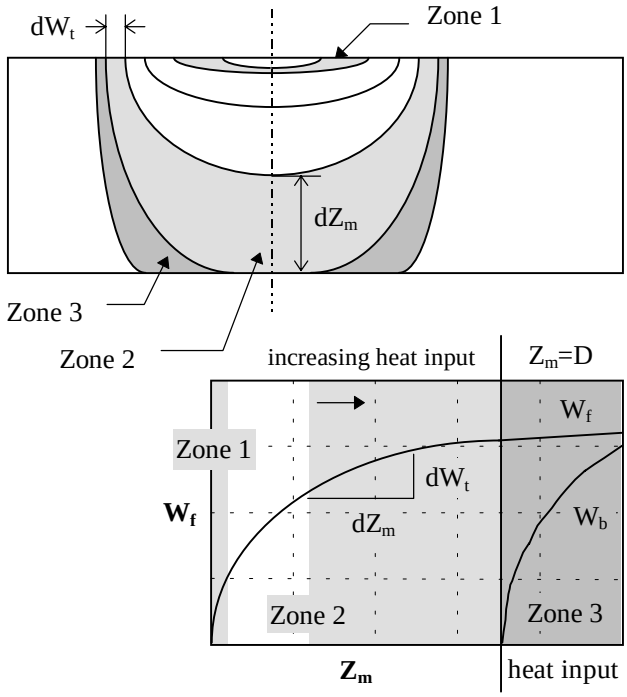

Fig. 13 Weld bead variations (heat conduction models)

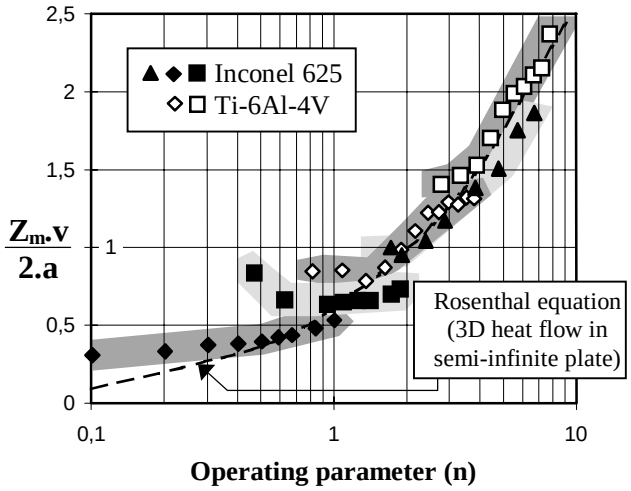

Fig. 14 Normalized weld penetration as a function of operating

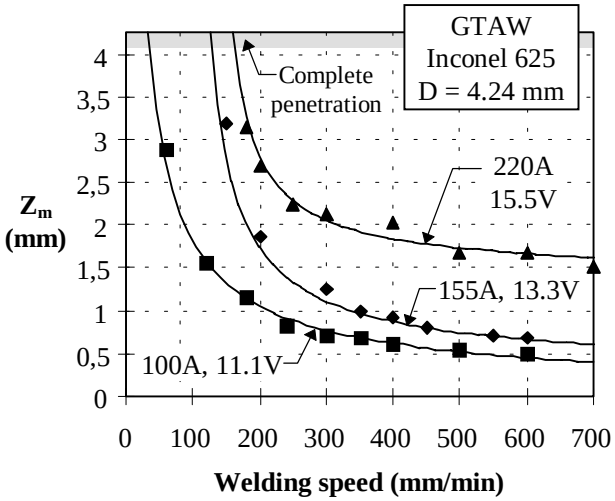

Fig. 15 Influence of the welding speed (v) on the penetration (Z_m) for Inconel 625

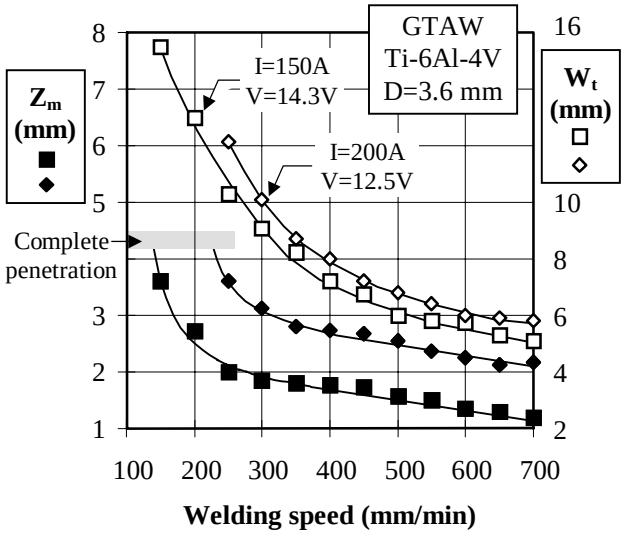

Fig. 16 Influence of the welding speed (v) on the weld penetration (Z_m) and weld width (W_f) for Ti-6Al-4V

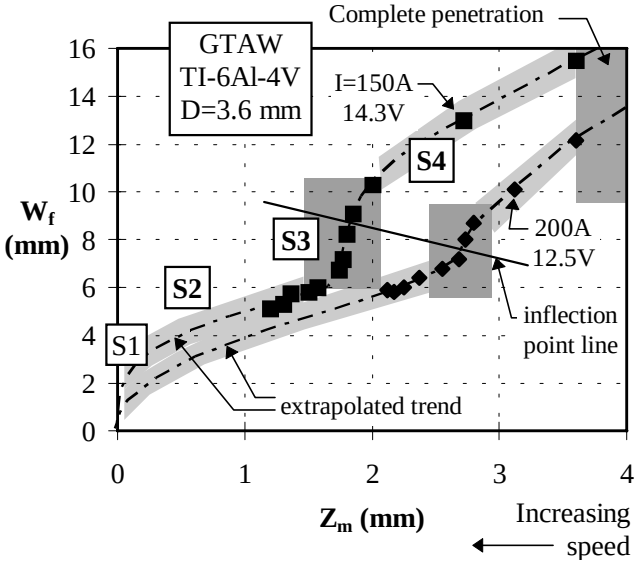

Fig. 17 Weld width (W_f) as a function of weld penetration (Z_m) for various welding parameters for Ti-6Al-4V

high current and complete penetration is much steeper for Inconel 625. In the previous discussion, it was pointed out that weld bead widths are not subjected to similar variations near complete joint penetration. In fact, a similar sensitivity is found for weld bead widths, as illustrated in Fig. 16. Further deviation from the calculated trends can be detected by looking at the variation of one weld bead dimension as a function of another, as shown in Fig. 17.

The deviation from the trends predicted by the heat conduction model (Fig. 17 and 13) can hardly be separated from the weld pool convective flows. In Fig. 17, four discernible stages that can be associated to changes in the heat transfer mechanism have been indicated by the letter S followed by a number between 1 and 4. At the higher welding speeds that only yield a surface melting (S1), the heat conduction undoubtedly plays a dominant role because of the relatively small size and small thermal inertia of the weld pool. At this very first stage, the cooling is so severe that it does not give sufficient time for convection to contribute in an appreciable way. The heat flow is then three-dimensional, and the heat extraction efficiency is maximized. In the ultimate stage (S4) that occurs near complete joint penetration, conduction acquires once again a significant effect despite the important role played by the weld pool convection. A large part of the heat arriving on the backside is reoriented to the weld pool by conduction. In stage 2, and especially 3, convection clearly gains importance with respect to conduction.

It has been mentioned earlier that the heat input, defined as q/v, is a meaningful parameter under particular conditions. For a heat transfer controlled by conduction, an invariant q/v is expected to produce very similar effects, if the thickness contribution is reduced to zero and the arc length (heat source size) is kept constant. However, nonnegligible variances can exist between welds performed at identical heat inputs. As shown in

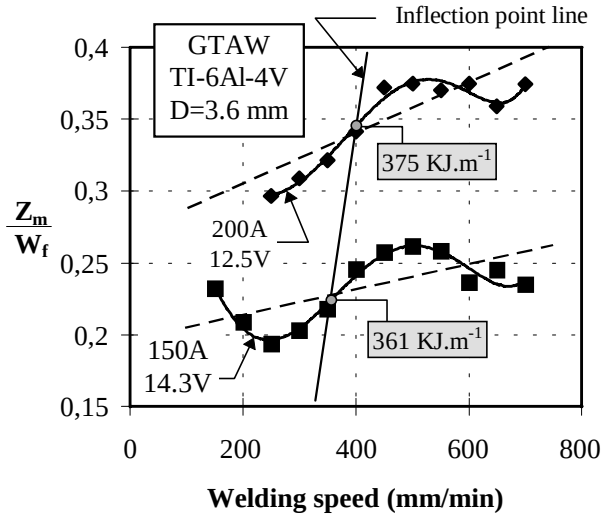

Fig. 18 Weld aspect ratio (Z_m/W_f) as a function of welding speed for two heat inputs for alloy Ti-6Al-4V

Fig. 18, the weld penetrations are deeper at high current while the weld widths are noticeably reduced; thus, Z_m/W_t is enhanced. The influence from both the Lorentz electromagnetic force and arc pressure that increases with current is clearly shown. In Fig. 17, two inflection points that characterize the dimensional behavior of the pool are noticed. In Fig. 18 where the same inflection points are reproduced, it is found that they take place at comparable heat inputs (q/v). As the current increases, the curve inflection is markedly reduced as a result of an increasing vertical force acting on the weld pool (Fig. 17). On the contrary, the curve inflection is accentuated when the current is lowered. A force that acts against the Lorentz force and that can only be attributable to surface tension gradients is therefore acquiring importance (Fig. 2). The resulting Marangoni flow (outward) shows that, under the imposed experimental conditions, Ti-6Al-4V alloy exhibits a negative surface tension gradient ($d\gamma/dT$). Because this flow appears to predominate at an approximately constant heat input, it is reasonable to assume that the weld pool central temperatures are then in the same order of magnitude, and so, the Marangoni flows then detected are probably also very similar.

5. Conclusions

Substantial weld bead variations are frequently observed in the proximity of complete penetration. The fundamental explanation of this variability must be attributed to heat flow changes resulting from welding variable fluctuations, thickness variations, or edge effect. As complete penetration approaches, the heat flow rapidly changes from the three-dimensional to the less-efficient two-dimensional. During this transition, any weld variable changes, even considered insignificant, can have an important effect on the weld bead morphology. Therefore, as explained using a dimensionless approach, any alteration of q^* or v^*, that is, welding power (q), welding speed (v), heat source radius (R), must be avoided in this transition regime. The use of the concept of relative plate thickness (τ), introduced by Jhaveri, has allowed the determination of this transition heat flow. A new dependence among the relative plate thickness, the heat source size, and the plate thickness has been found. The trends predicted by the model have been experimentally verified. However, some discrepancies have been encountered. In the Ti-6Al-4V alloy, the factor that gives rise to such variability has been identified as surface tension. It produces a considerable outward flow, which can be reduced when applying increasing downward forces, that is by intensifying the welding current. A reduction of the surface tension induced flow, or Marangoni flow, seemingly restores the ability of the theoretical model to correctly predict trends in weld bead dimensions.

Acknowledgment

The authors would like to express their gratitude to Professors Glen Edwards, Stephen Liu, and David Olson from the Colorado School of Mines for the useful discussions of the topic and for reviewing the manuscript.

References

1. K. Ishizaki, *Proc. Int. Conf. on Arc Physics and Weld Pool Behavior,* TWI, Abington Hall, Cambridge, England, 1980, p 267-277
2. V.A. Bukarov, Y.S. Ishchenko, and V.G. Loshakova, *Svar. Proizvod.*, Vol 11, 1978, p 4-7
3. P. Burgardt and R.D. Campbell, *Key Engineering Materials, Ferrous Alloy Weldments,* Vol 69 and 70, D.L. Olson and T.H. North, Ed., Trans. Tech Publications, 1992, p 379-416
4. B.J. Bradstreet, *Weld. J.*, Vol 47 (No. 7), 1968, p 314s-322s
5. K. Ishizak, Dynamic Surface Tension and Surface Enthalpy Theory on Heat Transfer and Penetration in Arc Welding, IIW (International Institute of Welding) Doc. No. 212-736-89, 1989
6. S.K. Marya and D.L. Olson, *Mém. Étud. Sci. Rev. Métall.*, 1989, p 25-34
7. S.K. Marya, *Scr. Mater.*, Vol 34 (No. 11), 1996, p 1771-1745
8. P. Burgardt and C.R. Heiple, *Weld. J.*, Vol 71 (No. 9), 1992, p 341s-346s
9. T. Zacharia, S.A. David, J.M. Vitek, and T. Debroy, *Weld. J.*, Vol 68 (No. 12), 1989, p 499s-509s
10. S.J. Bless, IIW (International Institute of Welding) Doc. No. 212-235-90, 1990
11. K.C. Mills and B.J. Keene, *Int. Mater. Rev.*, Vol 35 (No. 4), 1990, p 185-216
12. C.R. Heiple and J.R. Roper, *Weld. J.*, Vol 61 (No. 4), 1982, p 97s-105s
13. B.J. Keene, K.C. Mills, and R.F. Brooks, *Mater. Sci. Technol.*, Vol 1, 1985, p 568-574
14. D. Rosenthal, *Weld. J.*, Vol 20 (No. 5), 1941, p 220s-234s
15. T.W. Eager and N.S. Tsai, *Weld. J.*, Vol 62 (No. 12), 1983, p 346s-355s
16. J. Goldak, M. Bibby, J. Moore, R. House, and B. Partel, *Metall. Trans. B,* Vol 17 (No. 3), 1986, p 587-600
17. J.W. Elmer, W.H. Giedt and T.W. Eager, *Weld. J.*, Vol 69 (No. 5), 1990, p 167s-176s
18. N. Christensen, V. Davies, and K. Gjermundsen, *B. Weld. J.*, Vol 12 (No. 2), 1965, p 54-75
19. S. Kou, *Metall. Trans. A,* Vol 13 (No. 3), 1982, p 363-371
20. H.R. Shercliff and M.F. Ashby, *Metall. Trans. A,* Vol 22 (No. 10), 1991, p 2459-2466
21. M. Marya and S.K. Marya, *Proc. First ASM Int. European Conf.*, (Madrid) ASM International, 1997, p 18-26
22. P. Jhaveri, W.G. Moffatt, and C.M. Adams, *Weld. J.*, Vol 41, 1962, p 12s-16s
23. Chapter 3, *Welding Handbook*, 8th ed., Vol 1, American Welding Society, 1987, p 66-87